# Study of imploding detonations with high-speed videography and digital open-shutter photography

Sebastian Rodriguez Rosero[1], Jason Loiseau[2], Andrew J. Higgins[1]

[1] Department of Mechanical Engineering, McGill University
Montreal, QC H3A 0G4,CA

[2]Department of Chemistry and Chemical Engineering, Royal Military College of Canada
Kingston,ON K7K 7B4,CA

## 1   Introduction

Implosion of gaseous detonations is an interesting problem in detonation dynamics: As a detonation is focused into a progressively smaller region, it increases in strength, theoretically approaching a singularity at the center. As the strength of the wave grows, the detonation becomes increasingly over-driven and the cellular structure becomes finer; in theory, the detonation can become stable for sufficient degrees of overdrive. The implosion of gaseous detonations can be used for plasma generation, which has several applications.

From the seminal experimental study of Perry and Kantrowitz [1], it is known that the energy generated at the center of convergence of an imploding shock is in the form of a luminescence spot caused by a temperature increase in the order of 18,000 K [2], and an at least 18-fold pressure magnification in a quasi-stable implosion [3]. It is also known that the magnitude of the energy generated is dependent on the stability (or symmetry) of the converging front. In the case of imploding cylindrical detonations, transverse waves act as a distribution mechanism that attenuates the impact of local perturbations in the path of the wavefront; this distribution process allows for the transformation of polygonal shocks into cylindrical wavefronts given that the radius of the apparatus is sufficiently large as to permit enough time for the imperfections to disappear [4]. These findings are further supported by the theoretical modelling and numerical simulations in the recent work by [5], suggesting that cylindrical detonation fronts are largely stable, although this study did not incorporate multidimensional perturbations or the cell structure. Finally, a distinction between the stability of cylindrical detonation waves and cylindrical shock waves was made in [6] and confirmed by [7], as imploding cylindrical shock waves tend to be unstable and sensitive to local perturbations.

Since the early studies of [3], [4], and [6], the problem of stability of imploding gaseous detonations has not been examined with modern visualization techniques, such as ultra-high-speed videography and digital open-shutter photography. In this study, we will revisit the imploding detonation problem with state-of-the-art high-speed videography and multi-megapixel open-shutter photography.

## 2 Experimental apparatus

The implosion device was constructed out of 6061 aluminum and contains a 76-mm-high, 381-mm-wide cylindrical cavity with rounded edges. This design takes inspiration from the one built by Lee and Lee [3]. A 25-mm-thick center disk helps direct the detonation from the bottom of the cavity to the top, where it converges right below a 45-mm-wide quartz window. At the center of convergence, there is an aluminum insert that sits flush within the center disk, this insert is replaceable to suit different experiments. As seen in figure 1, the detonation originates at the pre-detonator (described below) and travels through a 9.5-mm-inner-diameter tube until it enters the cavity. The gas handling system is also displayed in the figure. Note that the apparatus was mounted atop of an aluminum extrusion structure anchored to the floor and isolated via vibration dampeners.
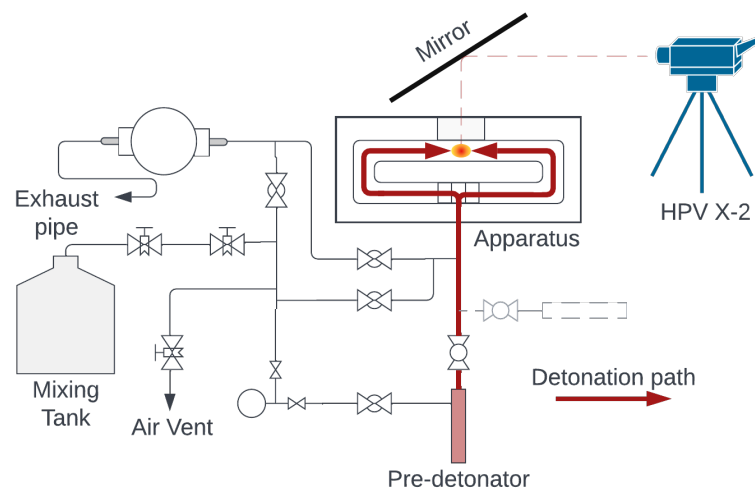


Figure 1: Schematic of the experimental setup and apparatus.

A wave-cutting insert was made to both limit the light intensity for open-shutter pictures and study the impact of the geometry of the test section in the stability of the wavefront. As seen in figure 2, the insert is mounted on the center disk, which leaves a small gap for the test section. The design displayed has a 200-mm-diameter, leaves a gap of approximately 4 mm and has a tapered side meant to redirect most of the detonation away from the test section. Also, the top was sandblasted and painted matte black to reduce light reflection. Other designs with varying diameter and height are currently being manufactured to further test the influence of the shape of the test section on the wavefront.
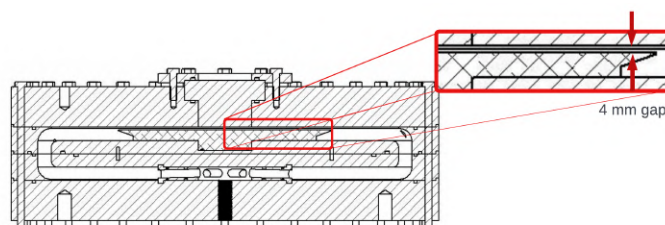


Figure 2: Render of the inside cavity with an insert in place.

To hold the center disk and allow the detonation to enter the chamber, two support configurations were tested. The first is a cylinder with six, equally spaced, diverging channels and the second corresponds to six airfoil-shaped supports. The different support pieces were used to test the impact of these in the

final implosion. As seen in the results section, these directly impact the profile of the converging wave. Figure 3 shows both support designs.
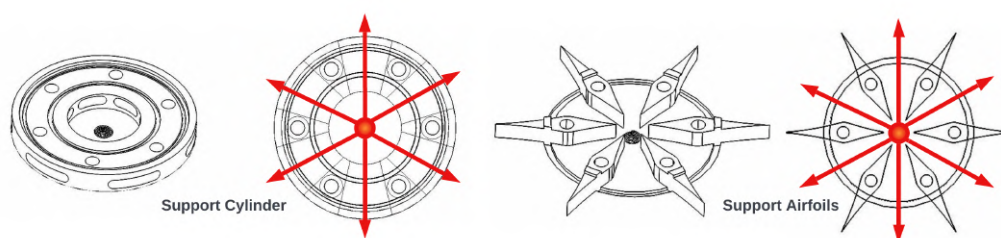


Figure 3: Support structure designs. Support cylinder (left) and airfoils (right). Red arrows symbolize the path of the detonation wave.

### 2.1 Pre-detonator

The ignition of the gas mixture is done with the use of a spark produced by a custom high-energy delivery system. The spark energy was not sufficient to achieve direct initiation or prompt DDT at low initial pressure (below 25 kPa). For this reason, a pre-detonator section was installed to improve the strength of the imploding detonation. This section consists of a 12.5-mm-wide and 381-mm-long cavity which is filled with the same gas mixture at a much higher initial pressure ($\approx$100 kPa) than the inside of the apparatus. Also, a Shchelkin spiral was added to promote the fast occurrence of DDT within this section. The pre-detonator is separated from the rest of the experiment by a 12.7-μm-thick Mylar diaphragm which is ruptured by the high-pressure wave created by the ignition.

## 3 Results

Both high-speed videography and open-shutter photography were used to visualize the implosion and the cell structure of the detonation. These were used to characterize the stability (symmetry) and location of the imploding detonation when subjected to different conditions such as different test section geometries, support configuration or initial pressure; initial pressure being proportional to the cell-size, which is believed to directly impact how sensitive a detonation is to perturbations.

### 3.1 High-speed videography

For these experiments, an equimolar acetylene-oxygen mixture at an initial pressure range between 10 kPa and 40 kPa was tested with a pre-detonator pressure of 100 kPa. The imploding detonation was recorded with a Shimadzu HPV-X2 camera at 2,000,000 FPS and 200 ns shutter speed. Camera was paired with a 75-300 mm Nikon lens and triggering was done with a PDA-55 photodiode pointed towards the window.

As seen in figure 4 below, the different support geometries influence the final shape of the wavefront. Particularly for the case when the support cylinder is in place (top of figure 4), the wavefront forms a six-sided polygon which matches the number of diverging channels in the support cylinder. On the other hand, with the airfoils the shape of the wavefront is largely uniform which is expected since the airfoils allow for a smoother recombination of the different wavefronts (separated by the supports). In either test, the wavefront is seen to be off centered with respect to the center of the test section and asymmetric.
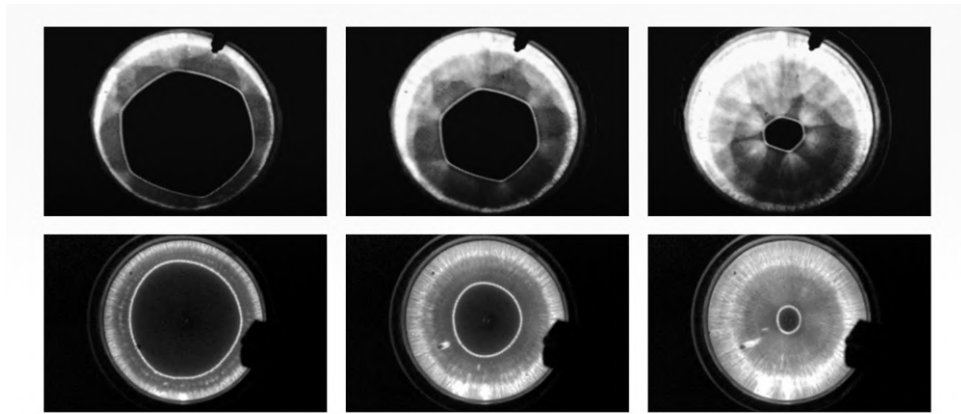
Figure 4: Video from two tests at 30 kPa with the disk insert in place. Top includes the support cylinder, bottom the support airfoils.

The asymmetry, off-center and azimuth of each detonation were extracted from the videos using a MAT-LAB script using an edge detection algorithm, based on [10]. The area, perimeter, and centroid of the wavefront were calculated from two different frames (three frames apart) and averaged. Then, the asymmetry was parameterized with the ratio $4\pi$ area/perimeter$^2$ which approaches unity as the wavefront approaches a circle. Furthermore, the off-center between the centroid of the wavefront and the center of the test section were measured while using a calibration of mm/px obtained from fitting the 45-mm-diameter window. Finally, the azimuth of the centroid with respect to the center of the test section was determined to record the exact position of the implosion center within the test section.

Since the extent of the interaction between the gas detonation and the apparatus depends on the cell size, initial pressure data was converted to cell-size for displaying the different measured parameters. The experimental cell-size data for equimolar acetylene-oxygen was obtained from [11] and a curve-fit was done to approximate the exact values corresponding to the measured range.

Several tests at each cell-size were done with the 4-mm-gap insert and the average of each parameter at each cell-size was computed and is displayed in figure 5, where the plots are respectively the average asymmetry, off-center, and azimuth for the different cell-sizes with error bars corresponding to the standard deviation. Note that only tests done with the airfoils were included in the plots.
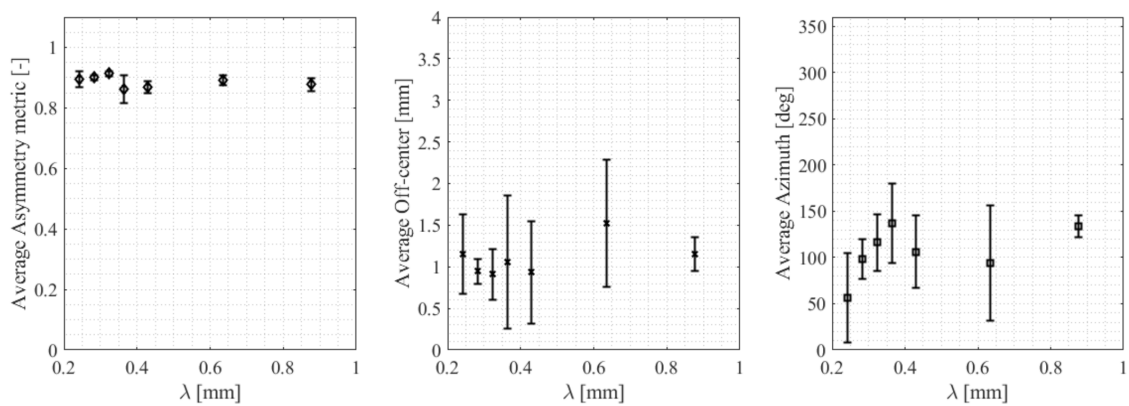


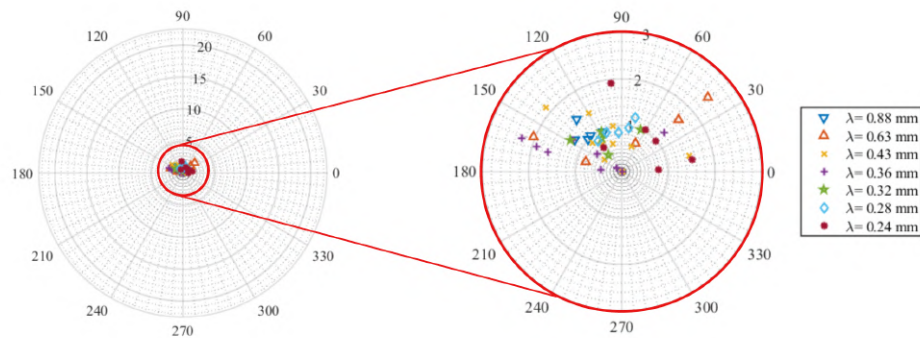Figure 5: Average asymmetry, off-center, and azimuth for a range of cell-sizes.

Figure 6: Recreation of the view from the window showing the location of the different tests.

As seen in figure 5, the detonation wavefronts are highly symmetric ,if the inherent cellular structure is neglected. At the same time, the off-center is fairly small with the maximum being approximately 2.5 mm with no relation to the cell-size detected. On the other hand, the azimuth of the centroid of the wavefront has a bias towards the upper hemisphere of the test section with most tests ranging between 50° to 150°. The bias in the azimuth for the different detonations is further displayed in figure 6. For this figure, the off-center and azimuth data were used to create a map containing the location of all the centers of implosion. For context, the graph on the left shows the different tests as seen from the 45-mm window and on the right, a close up to the area where all the results are located ( 6 mm wide).

The current hypothesis to explain these results links the azimuth bias with an inconsistency in the thickness of the test section, causing one side of the wavefront to travel faster than the other. This hypothesis is currently being tested by intentionally offsetting the wave-cutter and recording the effects this perturbation has on the detonation. Finally, it is speculated that some of the scatter seen in the data comes from when the planar detonation coming from the inlet pipe enters the cavity and strikes the center disk, which is expected to involve regular to Mach reflection transitions.

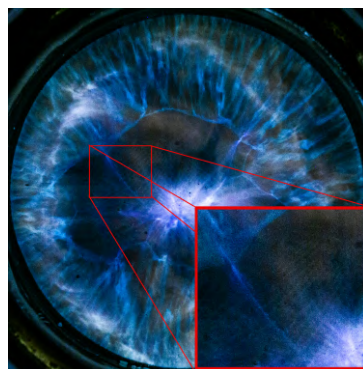## 3.2 Open-shutter photography



Figure 7: Cell structure as seen in the 15 kPa test.

For this experiment the technique from [12] was followed, with the difference that expanding cylindrical detonations were captured in their photographs, while the present study focused on the imploding geometry. The camera used was a Sony Alpha 6000 with a 2 s shutter time, f/5.6 and an ISO of 200.

Figure 7 shows the appearance of cells for the 15 kPa test. Several other images were obtained but are not included for the sake of brevity.

Images were post-processed to highlight the cellular structure of the detonation (seen in cyan and blue tones) and reduce the luminescence of reaction by-products (orange, magenta, and yellow tones). Current work includes the addition of a low-pass filter to produce cleaner images and lower pressure captures. Other gas mixtures may be used to improve the visibility of the cell structure.

# 4    Conclusion and further work

Preliminary results examining the implosion of gaseous detonation waves provide an interesting insight: First, it can be argued from the tests with different support conditions that the geometry of the apparatus will have a lasting impact in the shape of the wavefront until the point of convergence. Second, tests done within a 10-40 kPa pressure range show that under similar conditions, the symmetry of the wavefront is largely uniform, if the inherent cellular structure of the wave in neglected. Likewise, the off-center is small and no obvious relation with cell-size was found. On the other hand, a pattern in the angular location of the convergence point was seen and is believed to come from external factors related to inconsistencies in the geometry of the cavity. Finally, intentional perturbations and improvements to the test section geometry will be introduced to establish a parameter space for the different factors that influence the converging detonations.

# 5    Acknowledgements

# References

[1] R. W. Perry and A. Kantrowitz. 1951. The Production and Stability of Converging Shock Waves, Journal of Applied Physics, vol. 22, no. 7, pp. 878-886, https://doi.org/10.1063/1.1700067.

[2] T. Saito and I. I. Glass. 1982. Temperature measurements at an implosion focus.Proc. R. Soc. Lond. A384217–231. http://doi.org/10.1098/rspa.1982.0156.

[3] J. H. Lee and B. H. K. Lee. 1965. Cylindrical Imploding Shock Waves Physics of Fluids, vol. 8, no. 12, 1965, https://doi.org/10.1063/1.176117.

[4] R. Knystautas and J. H. Lee. 1971. Experiments on the stability of converging cylindrical detonations. Combustion and Flame, 16(1), 61–73. https://doi.org/10.1016/s0010-2180(71)80012-3.

[5] M. Short, G.J. Sharpe, V. Gorchkov, and J.B. Bdzil. 2005. Self-sustaining, weakly curved, imploding pathological detonation. Proceedings of the Combustion Institute, 30(2), pp.1899-1906. https://doi.org/10.1016/j.proci.2004.07.051

[6] R. Knystautas, J. H. Lee and J. H. S. Lee. 1969. Diagnostic Experiments on Converging Detonations. Physics of Fluids, 12(5), I–165. https://doi.org/10.1063/1.1692602.

[7] H. T. Wu, R. A. Neemeh, and P. P. Ostrowski. 1981. Experiments on the stability of converging cylindrical shock waves, AIAA Journal, vol. 19, no. 3, pp. 257-258. https://doi.org/10.2514/3.7770.

[8] S.I. Jackson and J.E. Shepherd. 2007. Toroidal imploding detonation wave initiator for pulse detonation engines. AIAA journal, 45(1), pp.257-270. https://doi.org/10.2514/1.24662.

[9] S.I. Jackson and J.E. Shepherd. 2008 Detonation initiation in a tube via imploding toroidal shock waves. AIAA journal 46, no. 9: 2357-2367. https://doi.org/10.2514/1.35569.

[10] MATLAB. 2021. Identifying Round Objects, The MathWorks Inc., Natick, Massachusetts,

[11] V. Manzhalei, V. Mitrofanov, V. Subbotin. 1974. Measurement of inhomogeneities of a detonation front in gas mixtures at elevated pressures, Combust. Explos. Shock Waves (USSR) 10 (1) 89–95.

[12] D. Qian, J. H. S. Lee and H. D. Ng. 2014. Formation and evolution of cylindrically diverging detonation waves in gases. Physics of Fluids, 26(9), 091103. https://doi.org/10.1063/1.4893538.